Journal of Physics: Conference Series

PAPER • **OPEN ACCESS**

Structure Analysis and Optimization Design of FDM Wire Extruder Screw

To cite this article: Bin Li *et al* 2021 *J. Phys.: Conf. Ser.* **1802** 022003

Structure Analysis and Optimization Design of FDM Wire Extruder Screw

Bin Li[1, 2, *], Peng Zhang[1], Hai Gu[1, 2], Jie Jiang[1, 2], Jianhua Sun[1], Yuanyuan Xu[1] and Jie Zhang[1, 2]

[1]School of Mechanical Engineering, Nantong Institute of Technology, Nantong Jiangsu, China
[2]Jiangsu Key Laboratory of 3D Printing Equipment and Application Technology, Nantong Jiangsu, China

*Corresponding author e-mail: libin19@ntit.edu.cn

Abstract. In order to improve the melt extrusion efficiency and extrusion stability of FDM wire extruder, ANSYS finite element software was used to analyze the flow field of the extruder screw. The effect of screw pitch, depth of screw groove, width of screw edge and length of metering section on velocity field, pressure field, temperature field and shear rate were studied by orthogonal test method, and the optimal combination of factors was obtained, then the optimized screw was tested and verified. The results show that when the screw pitch is 15mm, the depth of screw groove is 1.3mm, the width of screw edge is 1.5mm and the length of measuring section is 85mm, the wire extruder of FDM is smooth, efficient and safe.

1. Introduction

Fused Deposition Modeling (FDM) is one of the most widely applied 3D printing technologies at present, generally using ABS, PLA, PA and other thermoplastic wires [1]. FDM wire is mainly prepared by screw extruder. Screw is the most important part of FDM wire extruder, and its structure directly affects the quality and production efficiency of the extruder [2]. Therefore, it is necessary to optimize and analyze the screw structure, so as to improve the melt extrusion efficiency and extrusion stability of materials [3, 4].

Many scholars have studied the screw structure by numerical simulation. Ishkawa analyzed the distributive mixing performance of screw with different screw edge widths and lead angles, and the results showed that the forward, neutral and backward combination has significant distributive mixing performance, and the distributive mixing performance of the screw increases with the decreasing of the width of the screw edge [5]. Huang carried out simulation analysis on screw extruder through ANSYS software, and obtained the vibration mode of screw at each stage of natural frequency [6]. Guo established a mathematical model of the new screw with internal and external channels, and analyzed the fluid motion status and velocity streamline of the internal flow field, analyzed the macro pressure field and extruded performance [7]. Barrera used Ludovic software to calculate the two-dimensional flow field of power law fluid in the screw channel of a twin-screw thread element, and concluded that the pressure and temperature of the screw flow field were relatively stable [8]. Kim analyzed the non-Newtonian and non-isothermal flow with Carreau-Yasuda viscosity model in co-rotating and counter-

rotating twin screw extruder systems, and the mixing performances with respect to the screw speed, the screw pitch, and the rotating direction have been investigated [9].

This article aims to propose a best screw parameter of FDM wire extruder to yield optimal strew structure with Finite Element simulation. In this article combined effect of different screw pitch, screw groove depth, screw edge width and metering section length on screw flow field are analysed by orthogonal test method. On this basis, the screw designed by the combination of optimal factors is tested and verified, which provides a theoretical reference for the development of FDM wire extruder.

2. Theoretical model

2.1. Physical model

Main parameters of the screw as shown in Fig. 1, the screw thread length (L) is 255mm, the screw diameter (D) is 15 mm, the compression ratio (ε) is 3, the number of starts of thread (i) is 1, the lead angle (Φ) is 17.67°, the normal width of screw arris (w) is 1.5mm, the clearance distance between screw and barrel (δ) is 0.3 mm.

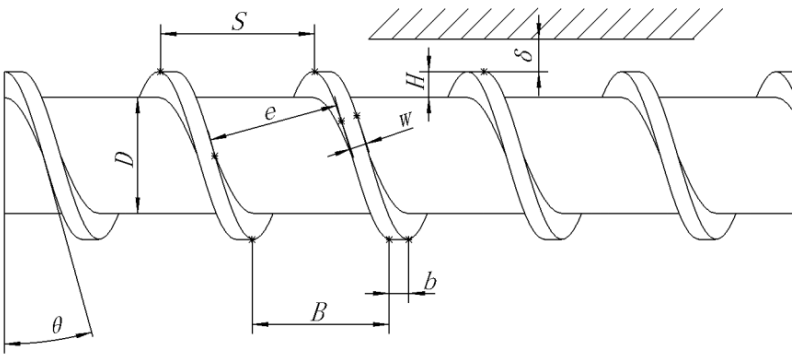

Figure 1. Geometric structure of screw.

The screw 3D model is created by SolidWorks software and shown in Fig. 2(a). The .x_t format file of the model is imported in ANSYS Workbench, and then for mesh generation. The meshed model consists of 892,077 elements with 183,367 nodes, as shown in Fig. 2(b).

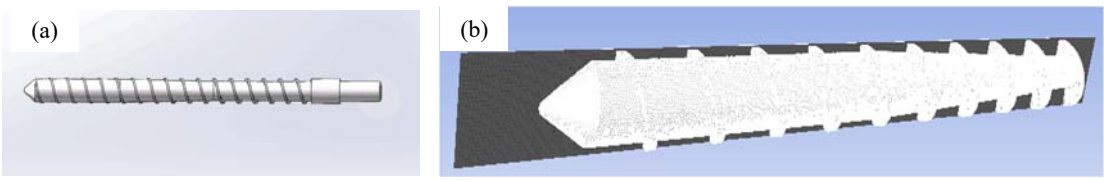

Figure 2. Geometry model and mesh generation. (a) Geometric model; (b) Mesh generation

2.2. Material parameter

ABS material was used in this simulation, and the properties of ABS are shown in Table 1, where ρ, c, k, T_m are the density, the specific heat capacity, the thermal conductivity, the melting point of ABS, respectively.

Table 1. The material properties of ABS.

Material	ρ/g·cm^{-3}	c/kJ·kg^{-1}·K^{-1}	k/W·m^{-1}·K^{-1}	T_m/K
ABS	1.05	2.24	0.03	540

2.3. Mathematical model

According to the technological conditions of screw extrusion and the properties of polymer, it is assumed that the temperature will change when the melt flows in the screw groove, and the effects of gravity, density, inertia force and viscosity of melt are ignored and the melt is incompressible during the flow. It is also assumed that the melt is in complete contact with the barrel and the screw groove, and no slippage occurs at the contact point between the screw edge and the barrel.

According to the above assumptions, the conservation of mass, conservation of momentum and conservation of energy equations can be simplified into Equations 1, 2 and 3, respectively.

$$\frac{\partial u}{\partial x}+\frac{\partial v}{\partial y}+\frac{\partial w}{\partial z}=0 \tag{1}$$

$$\begin{cases} \frac{\partial(\rho u)}{\partial t}+\frac{\partial(\rho uu)}{\partial x}+\frac{\partial(\rho uv)}{\partial y}+\frac{\partial(\rho uw)}{\partial z}=\frac{\partial}{\partial x}\left(\mu\frac{\partial u}{\partial x}\right)+\frac{\partial}{\partial y}\left(\mu\frac{\partial u}{\partial y}\right)+\frac{\partial}{\partial z}\left(\mu\frac{\partial u}{\partial z}\right)-\frac{\partial p}{\partial x} \\ \frac{\partial(\rho u)}{\partial t}+\frac{\partial(\rho vu)}{\partial x}+\frac{\partial(\rho vv)}{\partial y}+\frac{\partial(\rho vw)}{\partial z}=\frac{\partial}{\partial x}\left(\mu\frac{\partial v}{\partial x}\right)+\frac{\partial}{\partial y}\left(\mu\frac{\partial v}{\partial y}\right)+\frac{\partial}{\partial z}\left(\mu\frac{\partial v}{\partial z}\right)-\frac{\partial p}{\partial y} \\ \frac{\partial(\rho w)}{\partial t}+\frac{\partial(\rho wu)}{\partial x}+\frac{\partial(\rho wv)}{\partial y}+\frac{\partial(\rho ww)}{\partial z}=\frac{\partial}{\partial x}\left(\mu\frac{\partial w}{\partial x}\right)+\frac{\partial}{\partial y}\left(\mu\frac{\partial w}{\partial y}\right)+\frac{\partial}{\partial z}\left(\mu\frac{\partial w}{\partial z}\right)-\frac{\partial p}{\partial z} \end{cases} \tag{2}$$

$$\frac{\partial(\rho T)}{\partial t}+div(\rho uT)=div\left(\frac{k}{c_p}grad(T)\right) \tag{3}$$

Where u, v, and w are velocity components in the X, Y, and Z directions, respectively; C_p is specific heat capacity, T is temperature, and k is specific heat coefficient.

When analyzing the extrusion process of screw, the melt viscosity and the influence of temperature on the viscosity should be considered [10]. In present study, a non-Newtonian power ratio model is selected, and is given as

$$\eta=k(\lambda\dot{\gamma})^{n-1}\exp[-b(T-T_0)] \tag{4}$$

Where k is the viscosity coefficient; λ is melt relaxation time; $\dot{\gamma}$ is shear rate; n is the power law exponent; b is the temperature coefficient and T_0 is the reference temperature.

2.4. Boundary conditions

The flow channel is divided into four areas, namely, the outlet area, the inlet area, the inner wall and the outer wall, and the schematic diagram is shown in Fig. 3.

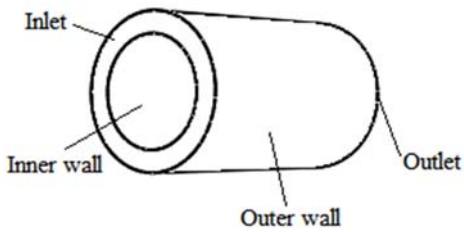

Figure 3. Schematic diagram of boundary conditions.

(1) Inlet boundary: The rate of inlet fluid is $0.27\times10^3 mm^3/s$, and the inlet temperature is 470K. (2) Outlet boundary: The melt velocity at the outlet is set as free extrusion, and the temperature is also set as free outflow. (3) Inner wall boundary: The inner wall is the part in contact with the screw groove. In the screw groove, the fluid needs to follow the screw to rotate, so a rotation axis needs to be set. The rotation speed is set at 20rad/s and the temperature is set at 470K. (4) Outer wall boundary: The outer wall is the surface in contact with the barrel. The boundary condition of velocity is 0, and the boundary temperature of the outer wall is set at 480K.

3. Optimization of screw structure

The optimal design of the screw is to conduct orthogonal test on the screw by changing four structural parameters, such as pitch, length of metering section, width of screw edge and depth of screw groove. The selected factors and levels are list in Table 2. The orthogonal table $L9(3^4)$ was used to simulate and analyze four indicators, including velocity, pressure, temperature and shear rate, and the experimental results are list in Table 3. Minitab version 17 software was used to analyze the data of the test results, and the influence trend diagram of each parameter was shown in Fig. 4.

Table 2. Test factors and levels.

Factor	Parameter	Level 1	Level 2	Level 3
A	Screw pitch/mm	14	15	16
B	Screw groove depth/mm	1.2	1.3	1.4
C	Screw edge width/mm	1.5	1.6	1.7
D	Metering section length/mm	83	84	85

Table 3. Orthogonal test scheme and results.

No.	A /mm	B /mm	C /mm	D /mm	Velocity /mm·s^{-1}	Pressure /MPa	Temperature /K	Shear rate /s^{-1}
1	14	1.2	1.5	83	19.5	19.7	461	135
2	14	1.3	1.6	84	19	19.3	460	143
3	14	1.4	1.7	85	20	18.9	463	169
4	15	1.2	1.6	85	21	20.1	466	162
5	15	1.4	1.7	83	21.5	20.7	464	137
6	15	1.3	1.5	84	24	20.6	470	105
7	16	1.2	1.7	84	22	19.5	467	139
8	16	1.3	1.5	85	22.5	19.2	465	142
9	16	1.4	1.6	83	23.5	18.8	463	153

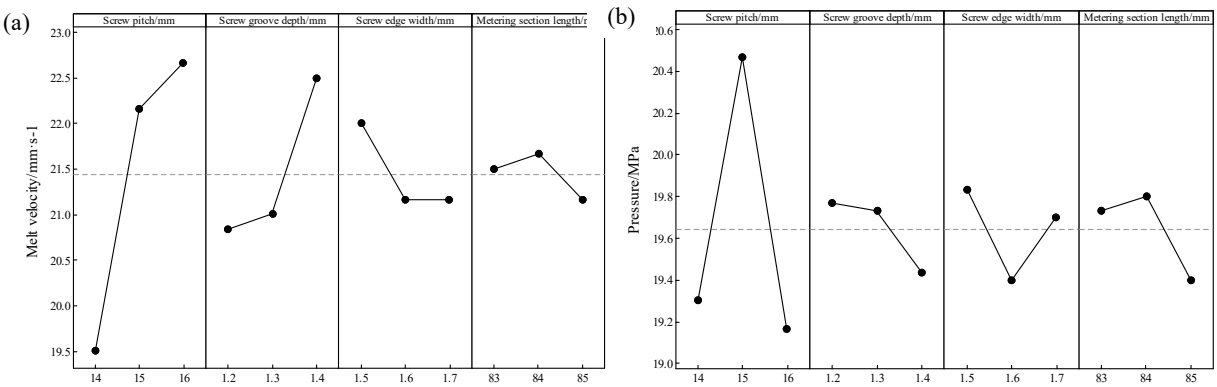

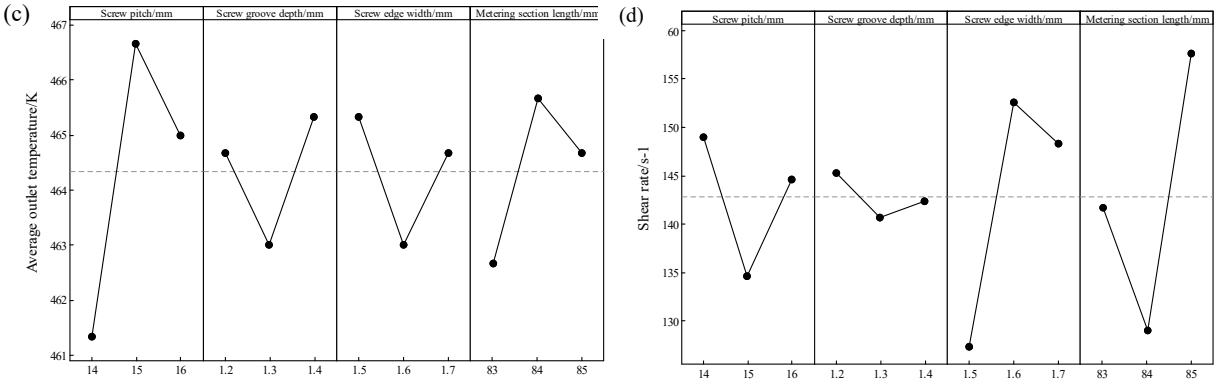

Figure 4. Indicator parameters influence trend. (a) effect on melt velocity; (b) Effect on the pressure; (c) Effect on average outlet temperature; (d) Effect on shear rate.

Combined with Table 3 and Fig. 4, it can be seen that the structural parameters of each group have a great influence on the pressure, with the maximum pressure reaching 20.7MPa and the minimum pressure only 18.8MPa, and the order of influence degree is $B_2>A_2>D_2>C_1$. The outlet temperature of each group is between 460K and 470K with little variation range. The higher temperature of outlet is favorable for wire extrusion, which can improve the extrusion efficiency of the wire, and the order of influence degree is $A_2>D_3>B_2=C_1$. The maximum shear rate of each group varied widely, ranging from $105s^{-1}$ to $169s^{-1}$. A smaller shear rate can make the extrusion more stable, and the order of influence degree is $D_3>C_1>A_2>B_2$. The melt flow velocity of each group varies greatly, ranging from 19mm/s to 24mm/s. Faster melt transport speed can speed up the extrusion speed, and the order of influence degree is $A_2>B_2=D_3>C_1$.

Based on the above analysis, the experimental combinations consistent with the optimization direction were determined, namely $A_2B_2C_1D_3$ with the highest melt extrusion temperature, the lowest maximum shear rate and the fastest melt transport efficiency, and $A_2B_2C_1D_2$ with the highest pressure. The excessive depth of the screw groove and screw pitch will affect the maximum pressure, and will also have a great change on the pressure during melt extrusion, which will eventually lead to the instability of wire extrusion and affect the quality of wire rod. Since a slight increase in the length of the metering section has little influence on the pressure, the optimal design scheme $A_2B_2C_1D_3$ was selected. The specific parameters were as follows: screw pitch was 15mm, depth of the screw groove was 1.3mm, width of the screw edge was 1.5mm, length of the metering section was 85mm.

4. Optimization result analysis

4.1. Velocity field analysis

The optimized overall velocity field distribution and axial distribution of the screw respectively is shown in Fig. 5. As can be seen from Fig. 5, the screw structure makes the melt flow velocity increase, and in the screw, groove is stable, and in the screw groove between the inlet of the compression section and the outlet of the metering section gradually and gently rises. The optimized maximum flow rate of melt in the screw groove reaches 28.5mm/s, and the conveying efficiency of the melt is greatly improved, which can improve the extrusion output and extrusion product quality. The melt flow velocity in the screw groove is stable, which reflects the stability of melt flow.

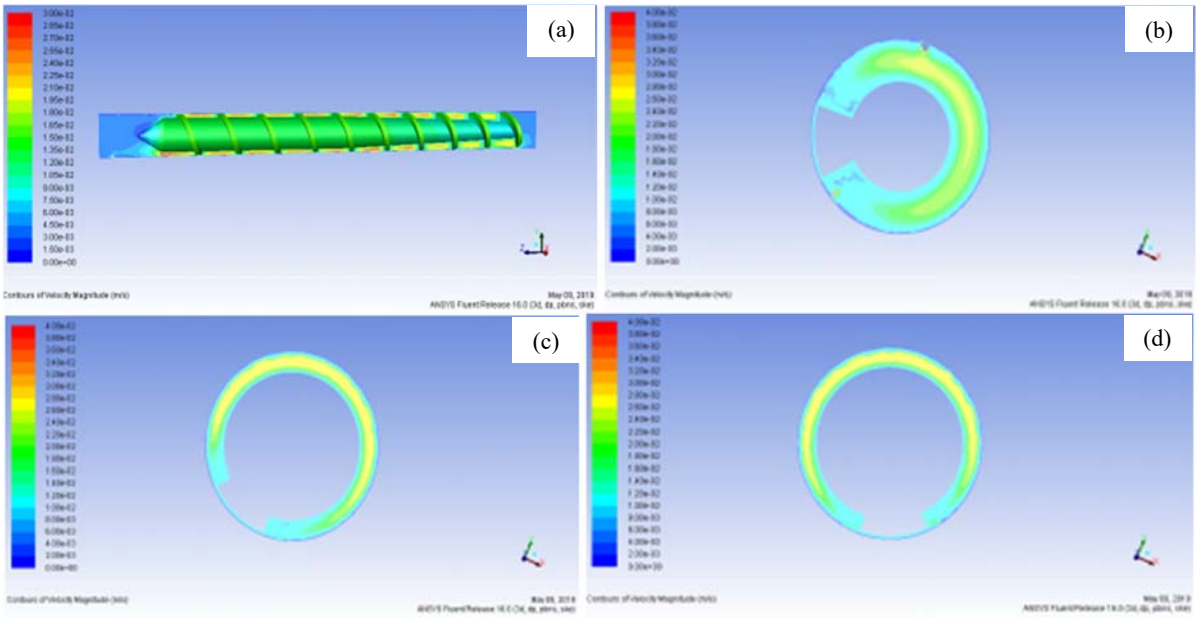

Figure 5. The optimized axial velocity field cloud. (a)overall; (b) compression section inlet; (c) compression section outlet; (d) metering section.

4.2. Pressure field analysis

The optimized overall pressure field distribution and axial distribution of the screw respectively is shown in Fig. 6. It can be seen from Fig. 6 that the maximum pressure of the screw is 20.6MPa. The melt pressure on the same section of the screw is very uniform. The melt pressure gradually decreases uniformly along the extrusion direction. the screw can bear more pressure and the pressure on the melt is more uniform, which is beneficial to melt extrusion.

4.3. Temperature field analysis

Fig. 7 show the optimized overall temperature field distribution and axial distribution of the screw, respectively. When entering the heating section, the melt temperature near the bottom of the screw groove is higher than in the screw groove. The melt temperature in the screw groove tends to be consistent, and the melt temperature difference in the screw groove decreases gradually. When it comes to the metering section, the melt temperature in the screw groove decreases. The average temperature of melt in the screw reaches up to 4.7×10^{2}K, which speeds up the melting velocity of the material and is more conducive to melt flow for more stable and efficient extrusion. The melt is uniformly heated in the screw groove, allowing for more efficient melting. The optimized screw can improve the melting efficiency of the material and make the melt transport faster.

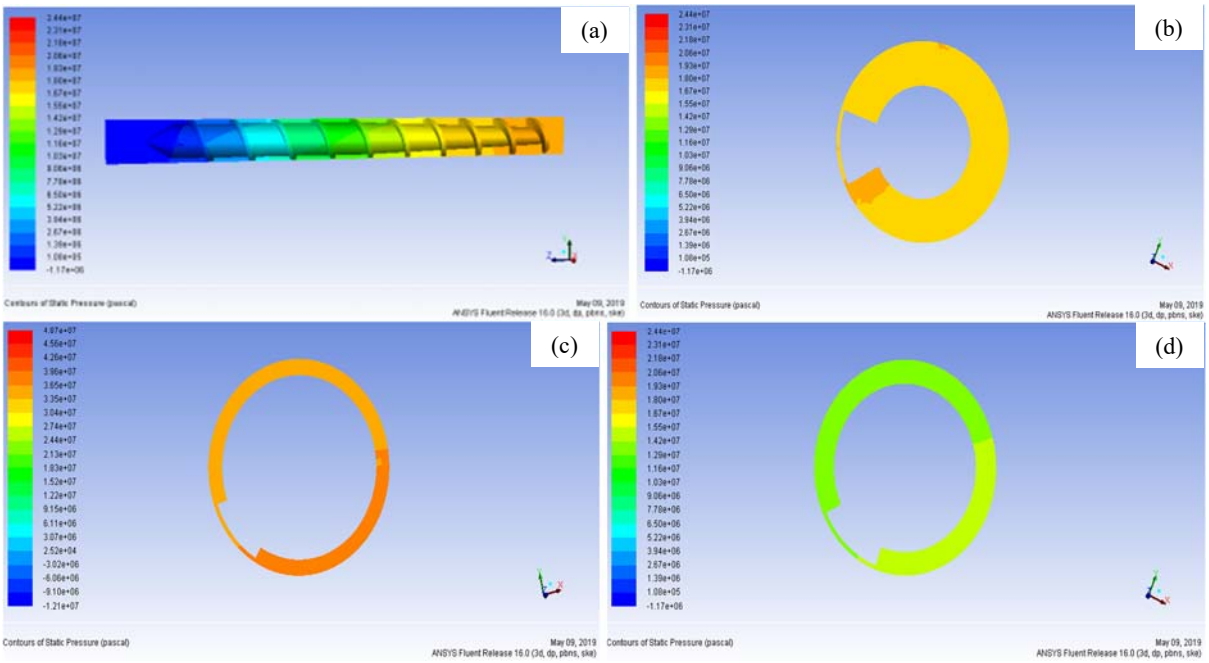

Figure 6. The optimized axial pressure field cloud. (a)overall; (b) compression section inlet; (c) compression section outlet; (d) metering section.

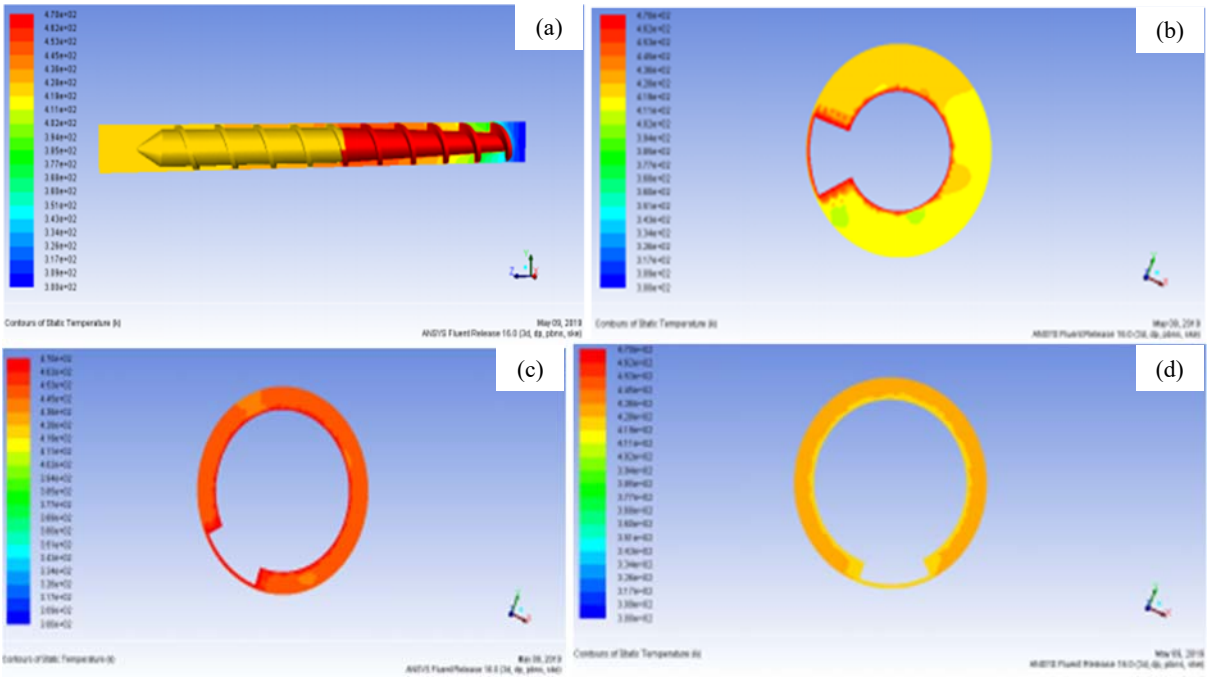

Figure 7. The optimized axial temperature field cloud. (a)overall; (b) compression section inlet; (c) compression section outlet; (d) metering section.

4.4. Shear rate analysis

The smaller screw shear rate is beneficial to the stability of melt flow, and the overall shear rate cloud of the optimized screw is shown in Fig. 8. The melt shear rate gradually increases from the compression section to the metering section as you can see from Fig. 8, and the maximum shear rate is $100s^{-1}$ at the

clearance between the screw edge and the barrel. The shear rate decreases gradually from the screw edge to the bottom of the screw groove, and the minimum shear rate is at the bottom of the screw groove.

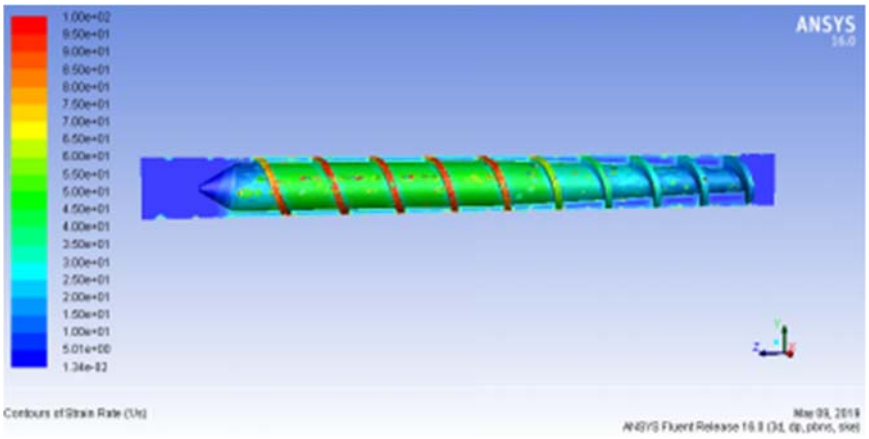

Figure 8. The optimized shear rate distribution cloud.

5. Conclusion

Flow field analysis and optimization design of different screw structures were carried out by ANSYS software. When the screw pitch is 15mm, the depth of screw groove is 1.3mm, the width of screw edge 1.5mm, and the length of metering section is 85mm, the screw structure makes the melt flow velocity increase, and the melt pressure decreases gradually from the compression section to the metering section. The melt temperature difference in the screw groove decreases gradually, and the melt temperature in the screw groove decreases to the metering section. The shear rate decreases and the melt extrusion becomes more stable. The optimized screw improves the melting efficiency of the material.

Acknowledgments

This work was financially supported by Young and Middle-aged Scientific Research Backbone Training Program of Nantong Institute of Technology (ZQNGG203), The Natural Science Foundation of the Jiangsu Higher Education Institutions of China (18KJB460023, 18KJA460006, 18KJD430006), Qinlan Program of Jiangsu Province (2019-3), Priority Discipline Construction Program of Jiangsu Province (2016-9) and Nantong Science and Technology Commission of China (MSZ18030) fund.

References

[1] Li B, Liu J, Gu H, et al, Structural Design of FDM 3D Printer for Low-melting Alloy, IOP Conference Series Materials Science and Engineering. 592 (2019) 012141.
[2] WANG Q, WANG Q, FANG H F, et al, The Numerical Simulation of Paper-Making Scraps Flow Field in Single-Screw Extruder Melt Conveying Section, Machinery Design & Manufacture. 2 (2018) 171 - 174.
[3] Chen K, Cui Y, Wang S, et al, Characterization of plasticizing process of single screw extruder with grooved melting zone, Journal of Polymer Research. 27 (2020) 1 - 11.
[4] Gao K Z, Hu D, Ding Y, et al, Effect of Extruder Screw Structure on PET Fiber Masterbatch Mixing Performance, Engineering Plastics Application. 47 (2019) 100 - 104.
[5] Ishikawa T, Kihara S I, Funatsu K, 3-D non-isothermal flow field analysis and mixing performance evaluation of kneading blocks in a co-rotating twin srew extruder, Polymer Engineering and Science. 41 (2001) 840 - 849.
[6] Huang Z G, Li M l, Yan M, et al, The Modal Analysis and Optimization Design of Single Screw Extruder, Shandong Chemical Industry. 45 (2016) 98 - 101.
[7] Guo S G, Zhang Z, Wang L Y, et al, Design and numerical analysis of the new type screw of single screw extruder, Feed Industry. 37 (2016) 10 - 13.

[8] Barrera M A, Vega J F, J. Martínez-Salazar. Three-dimensional modelling of flow curves in co-rotating twin-screw extruder elements, Journal of Materials Processing Technology. 197 (2008) 221 - 224.
[9] Kim N, Kim H, Lee J. Numerical analysis of internal flow and mixing performance in polymer extruder II: twin screw element, Korea-Australia Rheology Journal. 18 (2006) 153 - 160.
[10] Cunha G. Modelling and optimization of single screw extrusion. Lisbon: University of Minho, 1999.